

## Measurements of the Polarized ATR Spectra for Adsorbed Dye Layers by Using a Stack of Thin Glass Plates

Michio KOBAYASHI,\* Hitoshi TOKUNAGA, Jun OKUBO,<sup>†</sup> Toshihiko HOSHI,<sup>†</sup> and Yoshie TANIZAKI

Department of Chemistry, Nagaoka University of Technology, Nagaoka-shi 940-21

<sup>†</sup>Department of Chemistry, College of Science and Engineering, Aoyama Gakuin University, Chitosedai, Setagaya-ku 157  
(Received January 16, 1988)

Polarized ATR spectra have been measured for the dye layers adsorbed on stacked, thin glass plates. For the adsorbed Crystal Violet (CV) layer, the metachromasy band in the  $\parallel$  polarized ATR spectrum is blue-shifted and intensified in comparison with that in the  $\perp$  polarized ATR spectrum. This is in marked contrast to the observation for the adsorbed Methylene Blue (MB) layer that the  $\parallel$  polarized ATR spectrum is similar in shape and position to the  $\perp$  polarized ATR spectrum. The blue shift and the enhancement of the metachromasy band in the  $\parallel$  polarized ATR spectrum for the adsorbed CV layer is ascribed to an optical property characteristic of the adsorbed CV layer; the adsorbed CV layer exhibits an extra electronic transition band located at the high-energy side of the metachromasy band and polarized normal to the glass plane. Two possible explanations for the occurrence of this extra band are presented.

A conventional measurement of the absorption spectrum of molecules adsorbed on a glass surface using a polarized light with normal incidence allows only a two-dimensional detection of the optical anisotropy in the glass plane. In contrast, the polarized ATR (attenuated total reflection) method enables observations of the three-dimensional optical anisotropy of the adsorbed layer, including the anisotropy in the direction of the thickness.<sup>1)</sup> Wilks and Hirschfeld proposed a method for obtaining the ATR spectra by employing a stack of thin internal-reflection plates, the sample material being sandwiched between the plates.<sup>2)</sup> This method is ideal for liquids contained between the plates by capillary action. In the present study we measured the polarized ATR spectra in the visible region for adsorbed dye layers using a stack of thin glass plates whose surfaces adsorbed dye molecules.

### Experimental

Commercial Crystal Violet (CV) and Methylene Blue (MB) were used without further purification. A borosilicate glass plate (55×9.5×0.16 mm) was thoroughly washed by successive sonications in isopropyl alcohol, hot distilled water, concd nitric acid and hot distilled water and finally by steam washing with distilled water. Sixty sheets of the glass plates, thus cleaned, were placed in a holder appropriate for preventing stacking, and dipped in CV or MB aqueous solution for several hours. These glass plates which adsorbed CV or MB were, after rinsing several times with distilled water, placed in a plastic cell filled with distilled water, as illustrated in Fig. 1a. The polarized ATR spectrum for this sample cell was measured using a Shimadzu UV-360 spectrophotometer equipped with a Rochon-type polarizer made of synthetic quartz (Karl Lambrecht Corp.). The optical arrangement is shown in Fig. 1b. Ordinary rays from a Rochon-type polarizer are almost perfectly plane-polarized and the plane of their electric field vector can be rotated by rotating the polarizer. The  $\parallel$  and  $\perp$  polarized light thus obtained, the vibrating electric field vectors of which are parallel and perpendicular, respectively, to the plane of incidence, as defined in Fig. 1a, are introduced into the side of the stack of thin glass plates with an angle of incidence of  $\theta$ , defined in Fig.

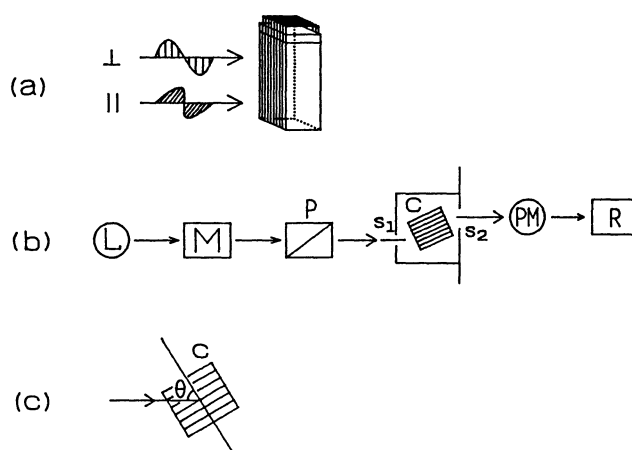


Fig. 1. Optical arrangement.

(a): definitions of the  $\parallel$  and  $\perp$  polarized lights. (b): optical path for the measurement of the polarized ATR spectrum. L: tungsten lamp, M: monochromator (prism+grating), P: Rochon-type polarizer,  $S_1$  and  $S_2$ : slit, C: cell containing a stack of thin glass plates, PM: photomultiplier, R: recorder. (c): definition of the angle of incidence ( $\theta$ ).

1c. Part of the incident light is scattered from the side surface of the glass plates, and a major part of the light entering the glass plates propagates within each plate, being totally reflected if  $\theta$  is larger than the critical angle ( $\theta_c = 61^\circ$  for the light passing from the glass layer to the water layer); the number of total reflections is about 20 for  $\theta = 70^\circ$  and about 10 for  $\theta = 80^\circ$ . In the case of these multiple total reflections, the  $\parallel$  ( $\perp$ ) polarized light remains  $\parallel$  ( $\perp$ ) polarized and the evanescent wave penetrates into the adsorbed dye layer; thus, the so-called  $\parallel$  ( $\perp$ ) polarized ATR spectrum for the adsorbed dye layer can be obtained. A correct, undistorted ATR spectrum can be obtained only when  $\theta$  is well above  $\theta_c$ .<sup>3)</sup> To compensate for the effect of light scattering from the glass surface and so forth, we used a reference cell which was identical with the sample cell, except that glass plates with no adsorbed dye layer were employed. As shown in Fig. 1b, we cut extraordinary rays from the Rochon-type polarizer by entrance slit  $S_1$  in order to avoid their disturbance on the ATR spectra, and admitted totally reflected ordinary rays

only to the detector by exit slit  $S_2$ , which was shifted in position from the entrance slit,  $S_1$ .

### Results

**Unpolarized and Polarized ATR Spectra of the Adsorbed CV Layer.** It is well-known that an aqueous solution of CV shows a metachromasy band in the visible region, with a shape and location which depends on the CV concentration, as shown in Fig. 2.<sup>4)</sup> With increasing CV concentration, the monomer band at 590 nm is weakened and a metachromasy band appears at 535 nm with an enhanced intensity.

We first confirmed that a reference cell containing 60 glass plates and filled with water gives no characteristic band and that the amount of the light loss is constant over the whole wavelength region examined, i.e., the absorbance of the reference cell was wavelength-independent, irrespective of the light polarization and  $\theta$ . Figure 3 shows the unpolarized ATR spectra for the adsorbed CV layer with several values of  $\theta$ . As  $\theta$  decreased, the metachromasy band at 526 nm was intensified to a greater degree than the monomer band at 590 nm. A correct, undistorted ATR spectrum giving a spectral pattern similar to the ordinary transmission spectrum was obtained when  $70^\circ \leq \theta \leq 80^\circ$  ( $\theta_c < \theta$ ).

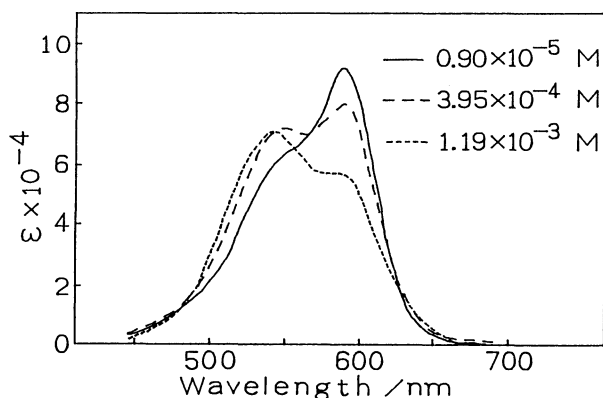


Fig. 2. Absorption spectra for the CV aqueous solutions of various concentrations.

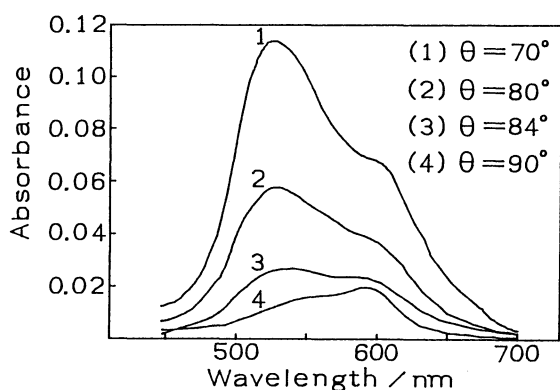


Fig. 3. Unpolarized ATR spectra for the adsorbed CV layer with several values of  $\theta$ .

Figure 4 shows the changes in absorbance at the band peak of the CV layer with respect to the adsorption time. According to the curve for  $\theta=0^\circ$  (normal incidence), the absorbance increased with increasing adsorption time. This means that the adsorption of CV molecules on the glass surface is not completed, even after 300 hours. In contrast to the curve for  $\theta=0^\circ$ , the absorbance is almost saturated in the curve for  $\theta=70^\circ$ . This may reflect some aspects characteristic of the ATR spectrum, i.e., the inapplicability of Lambert's law due to the attenuation or the finite penetration depth of the evanescent wave.

In Fig. 5 the unpolarized ATR spectrum for  $\theta=70^\circ$  is compared with the unpolarized transmission spectrum measured with  $\theta=0^\circ$  (normal incidence). On going from  $\theta=70^\circ$  to  $\theta=0^\circ$ , the absorbance increased as a whole; this seems to agree with the trend shown in Fig. 3. However, it should be emphasized that the peak position of the metachromasy band for  $\theta=70^\circ$ , 526 nm, is different from that for  $\theta=0^\circ$ , 535 nm. The spectrum for  $\theta=0^\circ$  in Fig. 5 agrees with that for a highly concentrated aqueous solution of CV regarding peak position

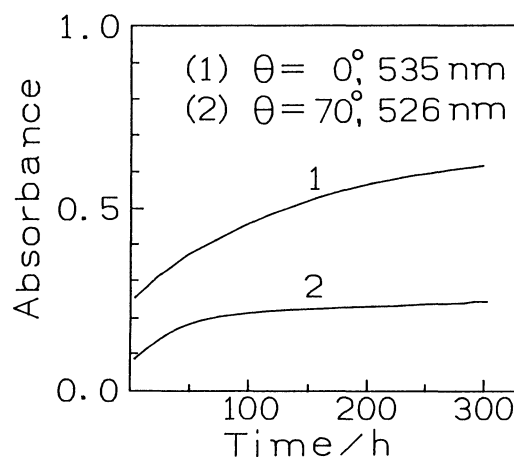


Fig. 4. Changes in the absorbance at the band peak of the adsorbed CV layer for  $\theta=0^\circ$  and  $70^\circ$  with respect to the adsorption time.

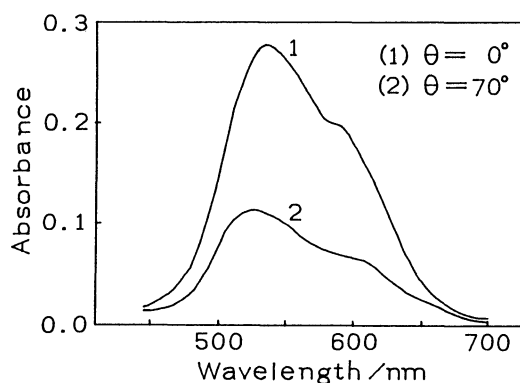


Fig. 5. Comparison of the unpolarized ATR spectrum of the adsorbed CV layer for  $\theta=70^\circ$  with the unpolarized transmission spectrum for  $\theta=0^\circ$ .

and shape.

The polarized transmission and ATR spectra measured for the adsorbed CV layer are summarized in Fig. 6. The essential coincidence of the  $\parallel$  and  $\perp$  polarized transmission spectra ( $\theta=0^\circ$ , Fig. 6a) implies that the adsorbed CV layer is optically isotropic within the surface plane of the glass plate. However, differences in the peak positions and absorbances are observed between the  $\parallel$  and  $\perp$  spectra for  $\theta=70^\circ$  and  $80^\circ$  (Figs. 6b and 6c). The differences are especially pronounced for  $\theta=70^\circ$ . The  $\perp$  polarized ATR spectrum for  $\theta=70^\circ$  (Fig. 6b) is nearly identical to the transmission spectrum ( $\theta=0^\circ$ , Fig. 6a), except for the band intensity (about twice), whereas the metachromasy band of the  $\parallel$  polarized ATR spectrum for  $\theta=70^\circ$  in Fig. 6b is largely blue-shifted in comparison with that of the  $\perp$  spectrum. This blue shift may be related to the origin of the difference in the peak positions observed in the unpolarized ATR and transmission spectra shown in Fig. 5. This blue shift is further enhanced with an increasing amount of adsorbed CV, as inferred from Fig. 6d.

**Unpolarized and Polarized ATR Spectra of the Adsorbed MB Layer.** Like CV, MB shows a metachromasy band at the high-energy side of the monomer

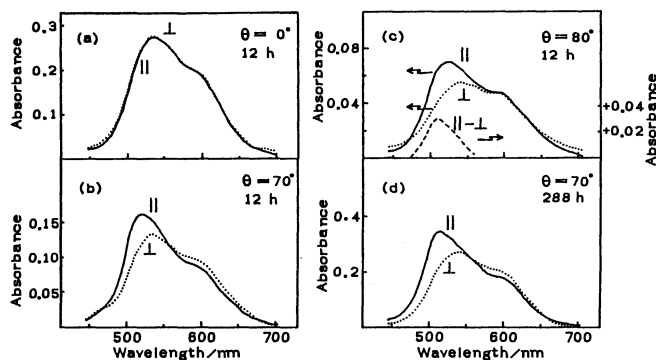


Fig. 6. Polarized transmission ( $\theta=0^\circ$ ) and ATR ( $\theta=70$  and  $80^\circ$ ) spectra of the adsorbed CV layer. The adsorption times are indicated.

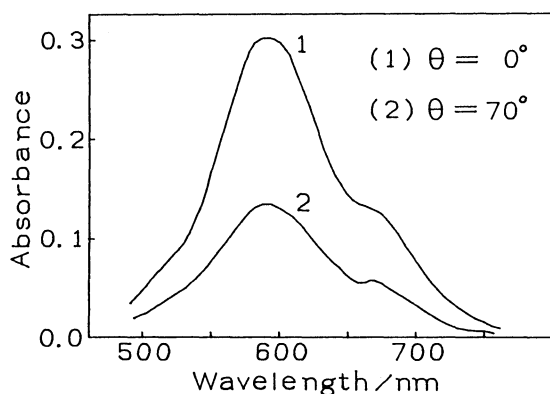


Fig. 7. Comparison of the unpolarized ATR spectrum of the adsorbed MB layer for  $\theta=70^\circ$  with the unpolarized transmission spectrum for  $\theta=0^\circ$

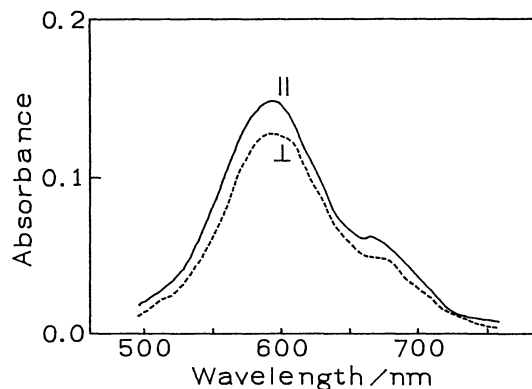


Fig. 8. Polarized ATR spectra of the adsorbed MB layer for  $\theta=70^\circ$ .

band in higher MB concentrations.<sup>5)</sup> In order to check whether the behavior of this ATR spectra is similar to that of the adsorbed CV layer, we measured the unpolarized and polarized ATR spectra of the adsorbed MB layer. The unpolarized ATR spectrum of the adsorbed MB layer measured with  $\theta=70^\circ$  is compared in Fig. 7 with the unpolarized transmission spectrum measured with  $\theta=0^\circ$  (normal incidence). In contrast to the unpolarized ATR and transmission spectra of the adsorbed CV layer shown in Fig. 5, the two spectra are quite similar and there is no difference in the peak positions. Figure 8 shows the polarized ATR spectra of the adsorbed MB layer for  $\theta=70^\circ$ ; the  $\parallel$  and  $\perp$  polarized ATR spectra are similar in shape, and the peak positions are coincident. This is, again, in marked contrast to the case of the adsorbed CV layer given in Fig. 6b or 6d.

## Discussion

For bulk materials or thick films, it is well-known that the  $\parallel$  and  $\perp$  ATR spectra are both red-shifted and that the longer-wavelength bands are relatively more intense in comparison with the ordinary transmission spectrum measured with normal incidence ( $\theta=0^\circ$ )<sup>6)</sup> by the following factors: (a) an anomalous dispersion in the refractive index,  $n$ ,<sup>7,8)</sup> and (b) a wavelength dependence of the penetration depth of the evanescent wave.<sup>9)</sup>

From the viewpoint of the general trend of the  $\parallel$  and  $\perp$  ATR spectra for bulk materials, the most remarkable features of the present observations are the differences in the polarized ATR spectra for the adsorbed CV (Fig. 6b) and the MB (Fig. 8) layers. As shown in Fig. 6b (CV), the metachromasy band of  $\parallel$  (520 nm) is blue-shifted from that of  $\perp$  (535 nm) and the intensity ratio of the metachromasy band to the monomer band for  $\parallel$  is larger than that for  $\perp$ . In contrast, the main feature of Fig. 8 (MB) is that the peak position of  $\parallel$  coincides with that of  $\perp$  and that the intensity ratio in question for  $\parallel$  is essentially equal to that for  $\perp$ . This feature of Fig. 8 excludes the possible influence of the

above-mentioned two factors that cause a deviation of the polarized ATR spectra from the transmission spectrum. This leads to the following conclusions: (1) The influence of non-total reflection<sup>7)</sup> due to the anomalous dispersion in  $n$  of an adsorbed dye layer is negligible for  $\theta=70^\circ$  in the case of the adsorbed MB layer, i.e., the dispersion in  $n$  of the adsorbed MB layer is not sufficiently large, even in the wavelength region of the absorption band, to influence the band location and intensity. (2) The evanescent wave penetrates the adsorbed MB layer perfectly, invalidating the wavelength dependence of the penetration depth of the evanescent wave. The former is in accordance with the known fact that the polarized and unpolarized ATR spectra of a thin film resemble its transmission spectrum unless there is a very strong dispersion in  $n$ ,<sup>10)</sup> as is the case for the adsorbed MB layer, which is considered to be a very thin film. The latter is also in accordance with the observation that the thickness of the adsorbed MB layer is estimated to be at most two or three molecular layers, if we assume that the molecular planes of MB are parallel to the surface of the glass plate. On the other hand, the penetration depth of the evanescent wave for visible light is several hundred Å; that is, the evanescent wave can penetrate into about one hundred molecular layers of the adsorbed MB.

As pointed out in the Results section, the  $\perp$  ATR spectrum for CV in Fig. 6b is considered to be equivalent to the transmission spectrum for CV in Fig. 6a measured with normal incidence. Therefore, the above-mentioned spectral features of the  $\parallel$  ATR spectra for the adsorbed CV layer concerning the location and intensity, in comparison with that of the  $\perp$  ATR spectra, are in marked contrast to those of the ATR spectra for bulk materials. This difference can be explained as follows: If there is a very strong dispersion in  $n$  of the thin film, the absorption maxima for the  $\parallel$  and  $\perp$  polarizations may not occur at the same wavelength; that is, the band for  $\parallel$  polarization is displaced to a shorter wavelength relative to the band for  $\perp$  polarization.<sup>10)</sup> If this is the case, the results in Fig. 6b could be explained as being due to a strong dispersion in  $n$  of the adsorbed CV layer. However, the following reasons can be used to eliminate this possibility. First, the magnitude of the molecular extinction coefficient ( $\epsilon$ ) in the visible region for CV ( $\epsilon=70000\text{--}92000$ ) is comparable to that for MB ( $\epsilon=60000\text{--}85000$ ). Second, the actual absorbance, i.e., the thickness of the adsorbed dye layer is also similar for CV and MB. Third, the degree to which the two bands in the visible region are overlapped is essentially the same for CV and MB, implying that there is no significant difference between CV and MB in the overlapping effect<sup>8)</sup> of the two anomalous dispersion curves in  $n$ . It must be recalled here that the peak for the  $\parallel$  ATR spectrum of CV adsorbed on an absorbing gold film electrode was blue-shifted from that of CV adsorbed on a transparent glass.<sup>11)</sup> That is, the pres-

ence of an extra absorption due to the gold film can cause a shift in the  $\parallel$  ATR spectrum of the adsorbed dye layer to a shorter wavelength. In conformity with this observation, we may conclude that the blue shift and the enhancement of the metachromasy band of the  $\parallel$  ATR spectra in Fig. 6b reflect an optical property characteristic of the adsorbed CV layer. We, thus, propose that the adsorbed CV layer exhibits an extra electronic transition band which is located at the high-energy side of the metachromasy band and is polarized normal to the glass plane. This extra electronic transition band can be detected only in the  $\parallel$  ATR spectrum, not in the  $\perp$  ATR spectrum nor in the transmission spectrum observed with  $\theta=0^\circ$ . We obtained this extra electronic transition band as a difference spectrum between the  $\parallel$  and  $\perp$  ATR spectra, as shown in Fig. 6c by the ( $\parallel-\perp$ ) curve.

There are two possible explanations for the occurrence of this extra electronic transition band under the assumption that CV molecules are adsorbed with their molecular planes parallel to the glass plane. First, CV has a nonplanar structure which gives rise to an out-of-plane polarized component of the electronic transition; it may, in turn, give rise to an extra electronic transition band polarized normal to the glass plane, under the present assumption. Second, the adsorption process gives an electronic perturbation to each CV molecule in the adsorbed CV layer to a different degree, being dependent on the distance from the glass plane, which may induce an intermolecular charge-transfer band with a nonvanishing intensity. In this charge-transfer band, the charge transfer occurs in the direction ( $z$ ) perpendicular to the glass plane; the transition moment should also be in the same direction.

We now give an explanation for the spectra shown in Fig. 3. With a decrease in  $\theta$  for  $90^\circ>\theta>\theta_c$ , the electric field amplitude of the  $\parallel$  polarized evanescent wave ( $E_\parallel$ ) increases to a larger degree than that of the  $\perp$  polarized evanescent wave ( $E_\perp$ ), although both  $E_\parallel$  and  $E_\perp$  increase.<sup>12)</sup> Among the electric field components of the evanescent wave that contribute to  $E_\parallel$ , especially the  $E_z$  component polarized perpendicularly to the glass surface increases in amplitude very sharply with a decrease in  $\theta$  for  $90^\circ>\theta>70^\circ$ .<sup>12)</sup> In conformity with this variation, the ATR spectrum for the extra electronic transition band, polarized perpendicularly to the glass surface and detected by the  $E_z$  component of unpolarized natural light, should increase in intensity with a decrease in  $\theta$  for  $90^\circ>\theta>70^\circ$ . The above change yields, along with an enhancement of the entire ATR band, an increase in the intensity of the metachromasy ATR band to a greater degree than the monomer ATR band with a decrease in  $\theta$ . There is, of course, the influence of an increasing number of total reflections with a decrease in  $\theta$  for  $90^\circ>\theta>70^\circ$ , which should also cause an enhancement of the entire ATR band.

The authors wish to express their thanks to

Professor Kozo Kuchitsu, Nagaoka University of Technology, for his critical reading of the manuscript.

#### References

- 1) N. J. Harrick, "Internal Reflection Spectroscopy," John Wiley & Sons (1967), p. 30.
  - 2) Ref. 1, p. 205; P. A. Wilks (Jr.) and T. Hirschfeld, Internal Reflection Spectroscopy, "Applied Spectroscopy Reviews," ed by E. G. Brame, Marcel Dekker, New York (1967).
  - 3) Ref. 1, p. 73.
  - 4) M. Schubert and A. Levine, *J. Am. Chem. Soc.*, **77**, 4197 (1955); L. V. Levshin and V. K. Gorshkov, *Opt. Spectrosc.*, **10**, 401 (1961); W. H. J. Stork, G. J. M. Lippits, and M. Mandel, *J. Phys. Chem.*, **76**, 1772 (1972).
  - 5) E. Rabinowitch and L. F. Epstein, *J. Am. Chem. Soc.*, **63**, 69 (1941); L. Michaelis and S. Granick, *ibid.*, **67**, 1212 (1945); E. Braswell, *J. Phys. Chem.*, **72**, 2477 (1968).
  - 6) Ref. 1, pp. 63—65 and 69—73.
  - 7) T. Fujiyama, "Bunkokagaku '68-B," the supplement 85 of "Kagaku No Ryoiki," ed by Y. Morino, T. Shimanouchi, S. Fujiwara, and M. Oki, Nankodo, Tokyo (1968), pp. 69 and 70; Ref. 1, pp. 83—87.
  - 8) T. Fujiyama, "Bunkokagaku '68-B," pp. 71 and 72.
  - 9) Ref. 1, Eq. 22 on p. 30.
  - 10) Ref. 1, pp. 68 and 69.
  - 11) W. N. Hansen, Internal Reflection Spectroscopy in Electrochemistry, p. 41, "Advances in Electrochemistry and Electrochemical Engineering (Vol. 9)," ed by P. Delahey and C. W. Tobias, John Wiley & Sons, New York (1973).
  - 12) Ref. 1, Fig. 10 on p. 29; Ref. 11, Fig. 3 on p. 16 and Fig. 4 on p. 17.
-